

# Multiphysics modelling of fractures in porous media using eXtended finite element method

A Jafari UNSW Sydney, and Gold Fields Australia Pty Ltd, Australia

M Vahab UNSW Sydney, Australia

N Khalili UNSW Sydney, Australia

## Abstract

Hydraulic fracturing is a technique used to increase the extent of rock fractures via injecting highly pressurised fluid. A key parameter controlling the efficiency of such a stimulation technique is to capture and minimise the amount of fluid leaked into the surrounding porous rock. In the current study, a novel fully coupled eXtended finite element method (XFEM) hydrofracture model is introduced to capture the effect of fluid loss on the efficiency of the fracturing treatment through the generalised leak-off model. In the proposed generalised leak-off model, the effect of the pressure drop on the hydrofracture faces and the associated decrease in the amount of leaked fluid is considered. The XFEM is then implemented into the COMSOL Multiphysics software package for the first time. The developed framework enables the handling of fractures simulations in complex scenarios particularly when various physics such as rock deformation, fluid flow and heat transfer are involved.

**Keywords:** COMSOL Multiphysics, XFEM, hydraulic fracturing, fractures, porous media

## 1 Introduction

Hydraulic fracturing is a versatile technique mainly used for the preconditioning mechanism in cave mining and stimulation of oil and gas reservoirs for enhancing production and recovery. During the course of hydraulic fracturing treatments, a high/large volume of pressurised fluid is injected into the rock formation for preconditioning purposes, in which the orebody is artificially weakened as a result of the de-stressing of the rock mass. such caving process can be either progressed by expanding pre-existing natural fracture networks or generating a new one (Jafari et al. 2021a). Inevitably, the efficiency of the fracturing job may be substantially reduced as a result of fluid leak-off into the surrounding porous media (Figure 1).

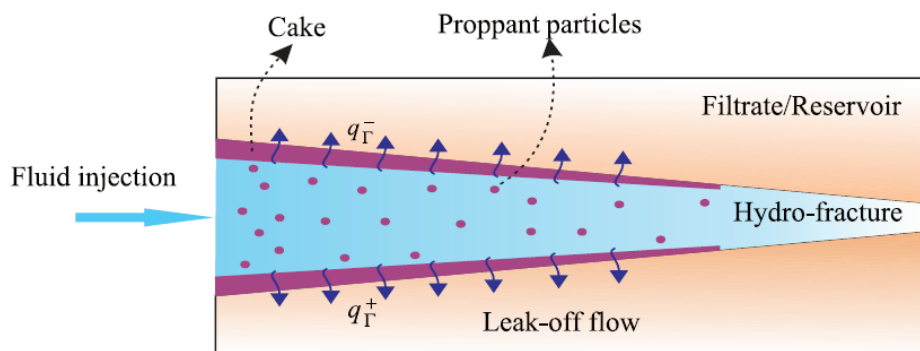


**Figure 1 Mechanism of the fluid leak during hydraulic fracturing (Jafari et al. 2021a)**

Over the past decades, concurrent experimental, analytical and numerical efforts were undertaken to develop predictive tools for the analysis of the role of discontinuities on the thermo-hydro-mechanical (THM) processes in deformable porous media (Terzaghi et al. 1996; Zienkiewicz et al. 1999; Khalili & Selvadurai 2003). With excellent inherent flexibility in tackling all types of discontinuities, computational superiority,

and other algorithmic advantages (e.g. circumventing the need for remeshing, data transfer, and mesh refinement for high gradients), the eXtended finite element method (XFEM) by Belytschko & Black (1999) has emerged as one of the most versatile tools for the study of discontinuities in deformable porous rock media.

Nevertheless, the application of XFEM to real-life engineering problems has been relatively limited, particularly with respect to the analysis of multiphysics processes in porous media. This has primarily been due to the fact that the majority of contributions in this context have been due to in-house codes with limited availability and capacity for handling complex geometries, large-scale domain and 3D analysis. COMSOL Multiphysics is considered one of the pioneering software packages which enables efficient handling of intricate coupling systems with enhanced efficiency and reliability. To date, COMSOL has been employed as a versatile platform for the phase-field implementation of a coupled hydro-mechanical analysis of porous media (e.g. see Zhou et al., 2018). However, no such extension of this powerful platform has been made to include XFEM within a multiphysics platform for multi-field practical solutions.

In this work, by taking advantage of the exceptional flexibility of this software in dealing with any arbitrary coupling processes, we present a THM framework for the XFEM analysis of discontinuities in deformable porous media. In this context, an exclusive XFEM framework for the study of THM coupling processes, compatible with the structure of COMSOL is introduced for the first time. The THM coupling process is carried out by exploiting the generic ‘Solid Mechanics’, ‘Darcy’s Law’ and ‘Heat Transfer in Porous Media’ physics interfaces in a conjugate manner to take account of the standard and enriched terms of the solution field. The proposed framework enables robust and efficient tackling of coupling systems with enhanced reliability in 2D/3D settings. The extended framework, in turn, facilitates the inclusion of further related physics as required.

## 2 Problem definition/formulation

In the case of thermo-hydro-mechanical modelling of fluid flow in porous media, the fully coupled model is constructed by means of three independent yet interacting sub-models Khoei et al. (2012); a poro-elastic model for the solid skeleton, a Darcy model for the fluid flow-through the pore devoid, and a heat transfer model for the pore-solid mixture. Hence, the governing equations of the problem are respectively as follow:

$$\begin{aligned}
 &\nabla \cdot \boldsymbol{\sigma} + \rho \mathbf{b} = 0 \\
 &\alpha \nabla \cdot \dot{\mathbf{u}} + \nabla \cdot \left( \frac{k_f}{\mu_f} (-\nabla p + \rho_f \mathbf{b}) \right) + \frac{1}{Q_t} \dot{p} - \beta_t \dot{T} = 0 \\
 &(\rho C)_{eff} \dot{T} + \rho_f C_f \left( \frac{k_f}{\mu_f} (-\nabla p + \rho_f \mathbf{b}) \right) \cdot \nabla T - \nabla \cdot (\lambda_{eff} \nabla T) = 0
 \end{aligned} \tag{1}$$

In the above, where  $\boldsymbol{\sigma}$  is the total Cauchy's stress,  $\mathbf{b}$  denotes the body force vector and  $\rho$  is the weighted average density of the mixture.  $\mathbf{u}$  is the displacement vector,  $k_f$  and  $\mu_f$  are respectively the intrinsic permeability of the domain and fluid viscosity,  $p$  is the pressure field,  $T$  denotes the temperature field, and  $Q_t$  and  $\beta_t$  are the compressibility and thermal expansion coefficients of the fluid. In addition,  $C_{eff}$  and  $\lambda_{eff}$  are the specific heat capacity and thermal conductivity of the medium. The schematic of the problem definition and the majority of terms/variables defined above are illustrated in Figure 2.

In the XFEM context and in order to derive the weak form of the governing equation, three sets of compatible test functions  $\boldsymbol{\eta}_u, \eta_p, \eta_T$  are adopted and multiplied by the corresponding governing equations.

By employing the Gauss-Divergence theorem, the weak forms are derived as follow:

$$\begin{aligned}
 \int_{\Omega} \nabla^s \boldsymbol{\eta}_u : \boldsymbol{\sigma} d\Omega &= \int_{\Omega} \boldsymbol{\eta}_u : \boldsymbol{\rho} \mathbf{b} d\Omega + \int_{\Gamma_t} \boldsymbol{\eta}_u \cdot \bar{\mathbf{t}} d\Omega \\
 \int_{\Omega} \eta_p \alpha \nabla \cdot \mathbf{u} d\Omega + \int_{\Omega} \nabla \eta_p \cdot \frac{k_f}{\mu_f} \nabla p d\Omega + \int_{\Omega} \eta_p \frac{1}{Q_t} \dot{p} d\Omega - \int_{\Omega} \eta_p \beta_t \dot{T} d\Omega &= \int_{\Gamma_{q_p}} \eta_p \bar{q}_f d\Gamma - \int_{\Omega} \nabla \eta_p \cdot \frac{k_f}{\mu_f} \boldsymbol{\rho}_f \mathbf{b} d\Omega \\
 \int_{\Omega} \eta_T (\rho C)_{eff} \dot{T} d\Omega + \int_{\Omega} \eta_T \left[ \rho_f C_f \frac{k_f}{\mu_f} (-\nabla p + \rho_f \mathbf{b}) \right] \cdot \nabla T d\Omega + \int_{\Omega} \nabla \eta_T \cdot \lambda_{eff} \nabla T d\Omega &= \int_{\Gamma_{q_T}} \eta_T \bar{q}_T d\Gamma
 \end{aligned} \quad (2)$$

As shown in Figure 2, the primary variables i.e. displacement, pressure and temperature fields are all considered to be potentially discontinuous across the fracture. Therefore, based on the XFEM, the primary variables fields can be approximated as

$$\begin{aligned}
 \mathbf{u} &= \mathbf{u}^{std} + H \times \mathbf{u}^{enr} \\
 p &= p^{std} + H \times p^{enr} \\
 T &= T^{std} + H \times T^{enr}
 \end{aligned} \quad (3)$$

Where  $\mathbf{u}^{std}$ ,  $p^{std}$  and  $T^{std}$  are the standard part, and  $\mathbf{u}^{enr}$ ,  $p^{enr}$  and  $T^{enr}$  are the enriched component of the displacement, pressure and temperature fields, respectively.  $H$  is the Heaviside enrichment function employed to implement the potential discontinuity across the fracture.

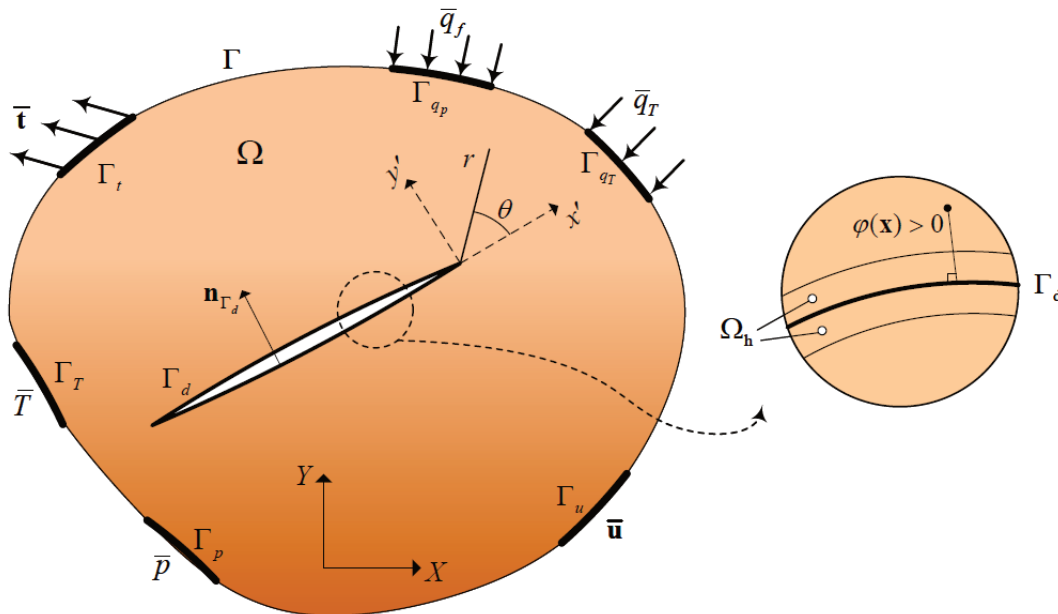


**Figure 2** Problem definition and boundary conditions

### 3 Implementation in COMSOL

COMSOL Multiphysics is a general-purpose simulation software for multi-field problems, that is based on the finite element method. In this software, multiple physics can be combined by employing the available built-in interfaces or implementing user-defined physics. The THM coupling analysis of fluid flow in deformable porous media, as shown in Figure 3, involves three distinct physics that take account of the mechanical deformation, fluid flow and heat transfer. In COMSOL, the 'Solid Mechanics' physics interface facilitates the most general toolkit to perform continuum-based structural analysis by solving the equations of motion endowed with suitable constitutive material behaviour. The fluid flow-through the porous domain

can be simulated via the Porous Media and Subsurface Flow module. In the case of low-velocity flows, which is commonly the case in geomechanics, then Darcy’s Law physics interface is employed to incorporate the flow-continuity equations within the porous medium. The Heat Transfer module offers heat transfer analysis in the host domain. For a detailed procedure of XFEM implementation of multiphysics fracture in COMSOL refer to Jafari et al. (2022, 2021b), as well as the numerical models available online at <https://github.com/ahmadjafari93/xfem-comsol.git>

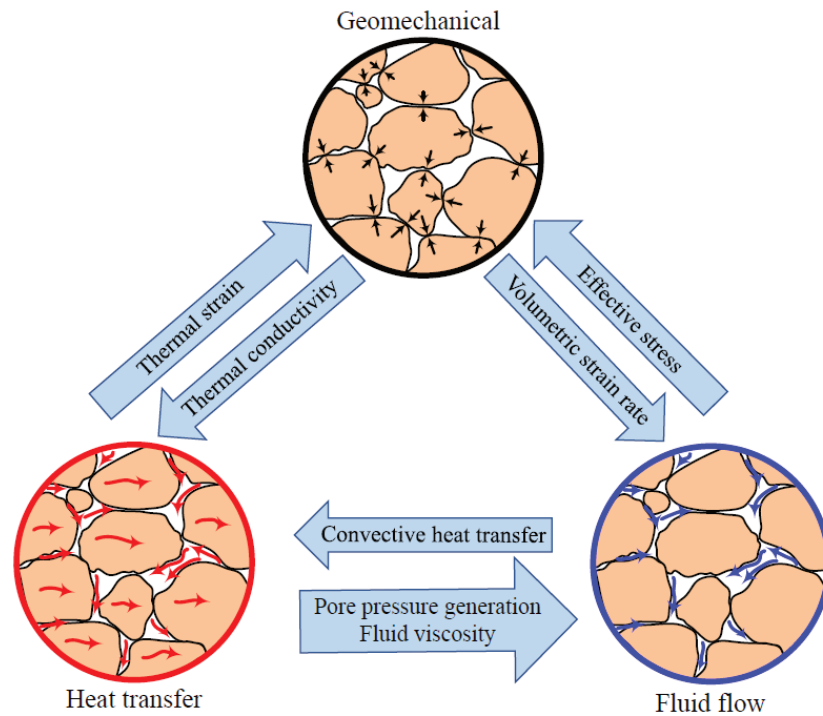


**Figure 3 Thermo-hydro-mechanical coupling flow chart (Jafari et al. 2021b)**

## 4 Numerical simulation results

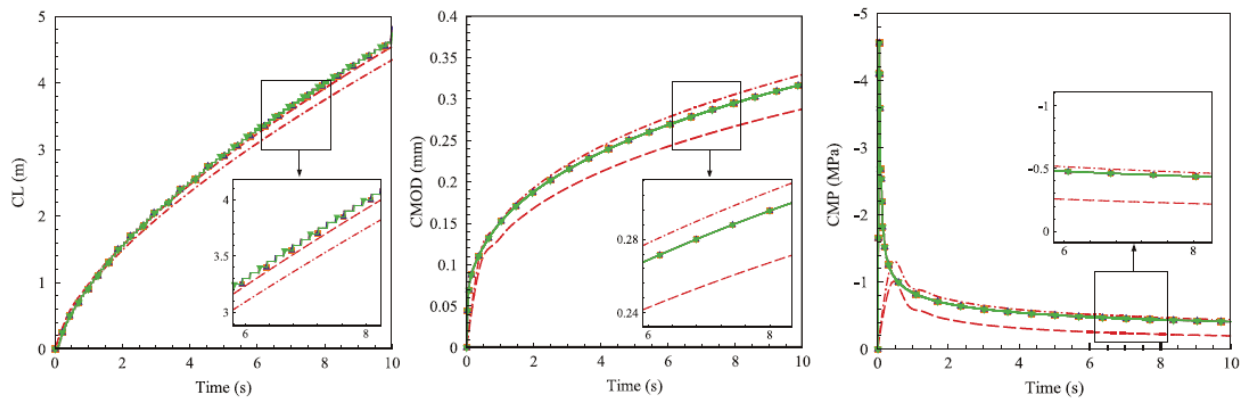
### 4.1 Hydraulic fracturing in semi-infinite domain

In this example, the well-known hydraulic fracturing closed-form solution by Geertsma & De Klerk (1969) and Spence & Sharp (1985) (a.k.a. the KGD problem) for an isolated hydrofracture subjected to a fixed injection rate in a semi-infinite impermeable domain is studied. In both simulation sets, the intrinsic permeability of the porous medium is assumed to be  $k_f = 10^{-16} m^2$ .

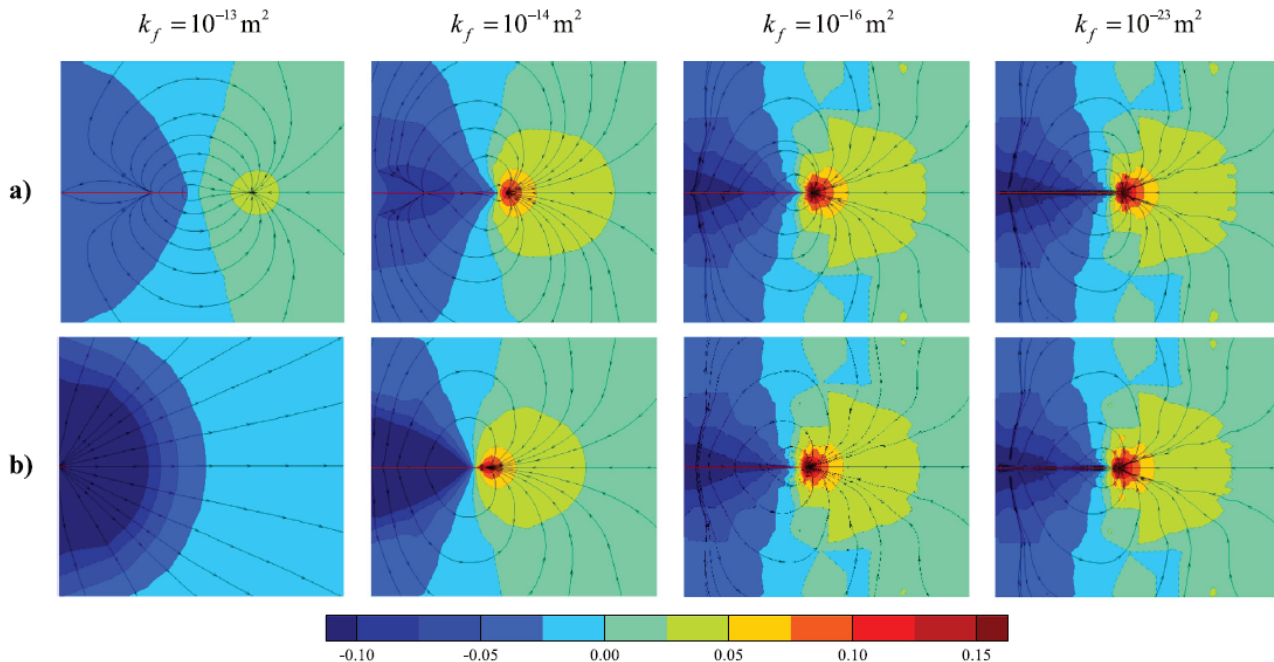
Figure 4 presents the variation with time of three main parameters of the hydro-fracturing simulation, namely the crack length (CL), crack mouth opening displacement (CMOD) and the crack mouth pressure (CMP). In all cases, an excellent agreement is observed between the solutions obtained through the proposed discontinuous pressure method, the continuous pressure method, and the analytical relationships. Note the formation permeability is assumed to be extremely low to resemble the impervious state that is assumed in the analytical solutions. Naturally, in this case, the intrinsic interfacial permeability induces no impact on the fracturing process. In addition, the different colours in the figure represent a sensitivity analysis of the proposed method with respect to the various interfacial permeability of the fracture. As shown, nearly all the simulation results are located in a narrow band and exhibit promising results.

Figure 5 shows the contours of the pore pressure at the final stage of simulation for both the discontinuous and continuous pressure descriptions. Note only the intrinsic interfacial permeability of 0 is considered here. For a relatively permeable medium; i.e.  $k_f = 10^{-13} m^2$ , the conventional approach predicts no pressure build-up due to intense leak-off of the fracturing fluid into the surrounding bulk medium. This, in turn, results

in the failure of the fracturing treatment since no fracture growth occurs. This is primarily confirmed via comparing the amount of the leaked water through the fracture aperture and the injected water, where the numbers are shown to be identical. However, this is in contrast with reality, as fracturing treatments are typically successful in this range of bulk permeability (Adachi & Detournay 2008). This is attributed to the formation of a cake layer along the fracture faces (Figure 1), which in turn dramatically reduces the treatment fluid leakage. In contrast, the approach presented here, which includes the effects of the cake layer, predicts reliably the pressure build-up as well as the pressure breakage due to the evolution of the cracks. Indeed, the inclusion of the interfacial permeability as a lumped factor appears to be a key effect in the simulation of the hydraulic fracturing treatments. Nevertheless, as the matrix permeability decreases to the impervious range, as expected, both simulation techniques converge to similar results and ultimately, in ideally impervious conditions, yield identical pressure distributions and hydraulic fracture lengths.



**Figure 4** Variation with time of a) Crack length (CL); b) Crack mouth opening displacement (CMOD); and c) Crack mouth pressure (CMP) using the proposed discontinuous method (Jafari et al. 2021a)



**Figure 5** Contours of pressure distribution for different permeabilities of the porous media using (a) The proposed discontinuous approach with no leak-off; (b) The continuous pressure model (the values are in MPa) (Jafari et al. 2021a)

### 4.2 Crack growth in 2D Solids

This example is adopted from Giner et al. (2009), which aims to investigate the effects of a hole in a rectangular plate on the crack propagation pattern. Figure 6 illustrates the geometry and boundary conditions of the plate, that is made of an aluminium alloy with  $E = 71.7 \text{ GPa}$  and  $\nu = 0.33$ . Consistent with the reference, the initial crack length and crack growth increment are set to 10 and 3 mm, respectively. An incrementally increasing traction is applied to the top edge of the plate with a maximum of 15 kN/m. The domain is discretised with 7,601 quadrilateral elements with an average element size of 0.67 mm.

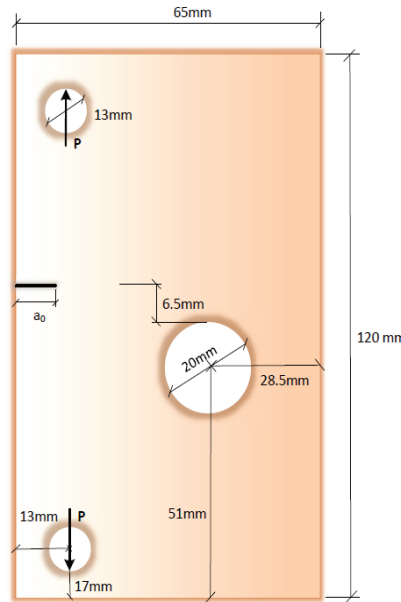


**Figure 6 Crack in a plate with hole – geometry and boundary conditions (Jafari et al. 2022)**

Figures 7a and 7b respectively show the crack trajectory and the von-Mises stress contour at the end of the analysis. The numerical results are in excellent agreement with the experimental observations as depicted in Figure 7c.

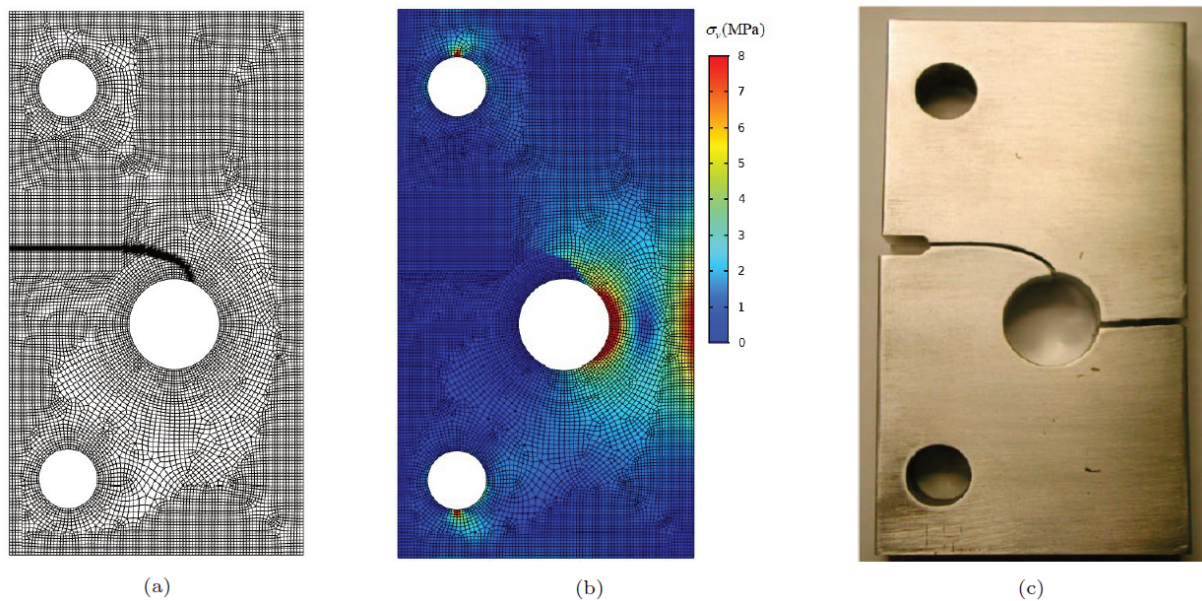


**Figure 7 Crack propagation in a rectangular plate with hole (a) Numerical crack path; (b) Von-mises stress contour at the end of simulation; (c) Crack trajectory based on experimental observations (Jafari et al. 2022).**

### 4.3 Randomly fractured porous media: two-dimensional THM analysis

Natural geological formations are heterogeneous and often contain numerous impermeable discontinuities and/or inclusions (e.g. hard rocks), which could be scattered throughout their bulk (Vahab et al. 2021). The following example illustrates the capability of the proposed implementation strategy in dealing with the simulation of multiple discontinuities in porous media (Figure 8). Boundary conditions are adopted as shown in Figure 8. A list of material properties is presented in Table 1. The domain contains 11 equally sized discontinuities with a length of 0.2 m each, which are studied for a total simulation time of 8,000 s. Figures 9a and 9b show the pressure and temperature contours at the end of the simulation. The promising performance of the strong discontinuity enrichment can be easily recognised across the discontinuities in both fields. The distribution of the heat flux accompanied by the flow streamlines is depicted in Figure 9c at the final stage of the analysis. Evidently, the fluid flow and the heat flux are both prevented across the contained adiabatic impermeable discontinuities, resulting in heat flux concentration at the crack tip zones.

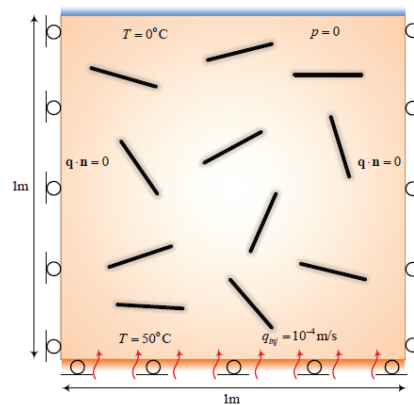


**Figure 8 Randomly distributed discontinuities in a porous medium: problem geometry and boundary conditions**

**Table 1 Material properties for the thermo-hydro-mechanical analysis of discontinuities in the porous medium**

Young's modulus, $E$ (GPa)	1.6
Poisson's ratio, $\nu$	0.33
Solid density, $\rho_s$ (kg/m <sup>3</sup> )	$2 \times 10^3$
Fluid density, $\rho_f$ (kg/m <sup>3</sup> )	$10^3$
Porosity, $n$	0.3
Bulk modulus of solid, $K_s$ (MPa)	$1 \times 10^{14}$
Bulk modulus of fluid, $K_f$ (MPa)	$2 \times 10^3$
Fluid viscosity, $\mu_f$ (Pa.s)	$2 \times 10^3$
Permeability, $k_f$ (m <sup>2</sup> )	$1 \times 10^{-12}$
Thermal conductivity of solid, $\lambda_s$ (W/m °C)	2.88
Thermal conductivity of fluid, $\lambda_f$ (W/m °C)	0.6
Solid specific heat capacity, $C_s$ (J/kg °C)	$1.17 \times 10^3$
fluid specific heat capacity, $C_f$ (J/kg °C)	$4.2 \times 10^3$
Volumetric thermal expansion coefficient, $\beta_s$ (1/°C)	$6.6 \times 10^{-6}$

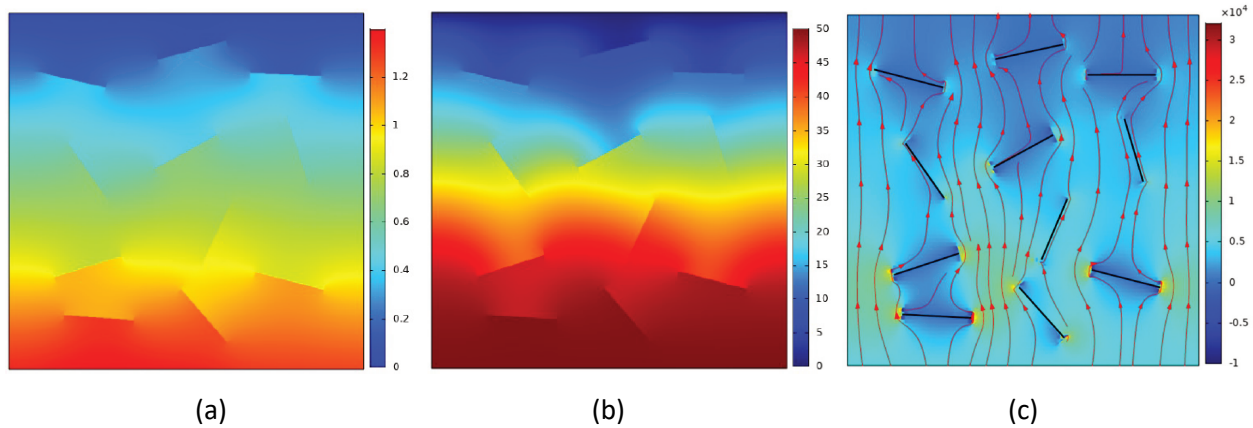


**Figure 9** The distribution contours of: (a) Pressure (MPa); (b) Temperature (°C); (c) Heat flux (W/m<sup>2</sup>) and associated streamlines at the end of THM analysis (Jafari et al. 2022)

#### 4.4 Fractured porous media: three-dimensional THM analysis

The final example is presented to show the general nature of the proposed THM XFEM framework for the study of three-dimensional problems in geomechanics. Suppose a cubic domain with a side length of 50 m that encompasses a penny-shaped impermeable discontinuity of diameter 20 m located at its centre (Figure 10). All material properties are the same as in the previous examples. The bottom surface is subjected to a prescribed temperature of 50°C and a constant inflow rate of  $10^{-4} \text{ m/s}$ , while both the pressure and temperature are assumed to vanish over the top surface (i.e.  $p = 0; T = 0$ ). The remainder surfaces are considered to be undrained, with no fluid flow/heat flux. All faces of the domain are constrained in their corresponding normal directions, except the top surface, so as to emulate the in situ boundary conditions. The porous domain is discretised using 2,312 brick elements, clustered in the vicinity of the internal discontinuity with an average element size of 1.5 m, in conjunction with 45,415 tetrahedral elements, elsewhere, that is simulated for the total duration of  $3 \times 10^5 \text{ s}$ . Figure 11 illustrates the contours of vertical displacement  $u_z$  as well as pressure and temperature fields, over two cross-shaped planes perpendicular to the discontinuity. Clearly, the discontinuity induced by the penny-shaped inclusion can be observed in all three distribution contours. This is further elaborated by noting the flow and heat flux streamlines that are depicted in Figures 11b and 11c, where a diversion from the far-field vertical alignment can be observed adjacent to the discontinuity region. The promising results presented here showcase the flexibility of the implemented technique in dealing with intricate scenarios in the 2D/3D thermo-hydro-mechanical analysis of porous media with single/multiple discontinuities.

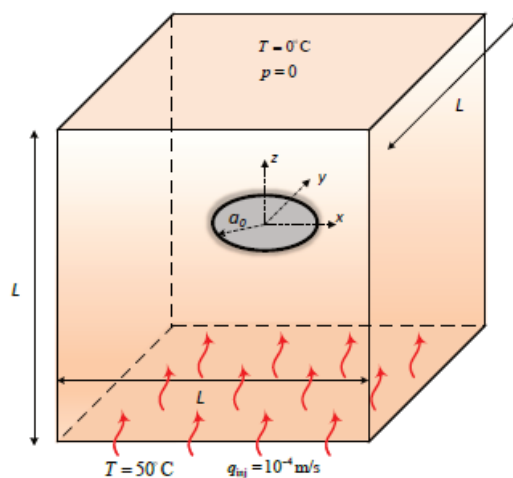


**Figure 10** Three-dimensional THM simulation of a fault in porous media; problem geometry and boundary conditions

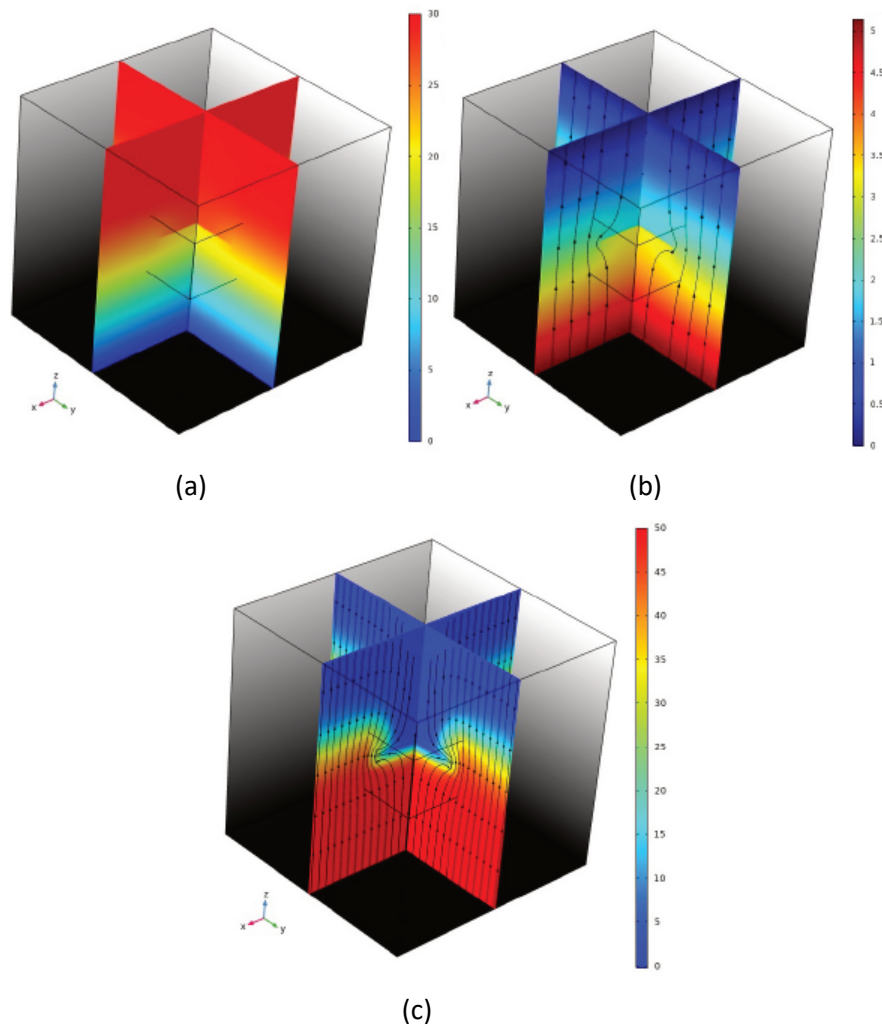


**Figure 11** 3D THM simulation results on two perpendicular planes. (a) Distribution of vertical displacement  $u_z$  (mm); (b) Pressure distribution (MPa) together with fluid flow streamlines; (c) Temperature distribution ( $^{\circ}\text{C}$ ) with heat flux streamlines

## 5 Conclusion

In this study, the hydraulic fracturing process, its associated fluid leak-off and implementation in the commercial software package COMSOL Multiphysics was introduced. To this end, the mechanism of fluid leak-off, which is widely overlooked in fully coupled numerical platforms, was introduced and its effects on the fracturing process were examined in the first numerical simulation. Then, the fully coupled formulation of a thermo-hydro-mechanical process in fractured porous media was introduced along with its first-time implementation procedure in COMSOL. To showcase the robustness and performance of the proposed framework, a series of uni-physics and multiphysics problems involving stationary and propagating fractures were employed in both 2D and 3D. The numerical simulation results indicate the capability of the proposed framework in dealing with complex fracture scenarios. Furthermore, the proposed platform can be further extended to account for more complex fracture scenarios (e.g. interacting fractures) and additional physics (e.g. chemical reactions) as required.

## Acknowledgment

The first author wishes to acknowledge the UNSW Sydney for funding the research conducted during the PhD program. The financial support provided by Gold Fields Australia for presenting the technical work is also acknowledged.

## References

- Adachi, JI, & Detournay, E 2008, 'Plane strain propagation of a hydraulic fracture in a permeable rock', *Engineering Fracture Mechanics*, vol. 75, no. 16, pp. 4666–4694.
- Belytschko, T & Black, T 1999, 'Elastic crack growth in finite elements with minimal remeshing', *International Journal for Numerical Methods in Engineering*, vol. 45, no. 5, pp. 601–620.
- Geertsma, J & De Klerk, F 1969, 'A rapid method of predicting width and extent of hydraulically induced fractures', *Journal of Petroleum Technology*, vol. 21, no. 12, pp. 1571–1581.
- Giner, E, Sukumar, N, Tarancón, JE & Fuenmayor, FJ 2009, 'An Abaqus implementation of the extended finite element method', *Engineering Fracture Mechanics*, vol. 76, no. 3, pp. 347–368.
- Jafari, A, Broumand, P, Vahab, M & Khalili, N 2022, 'An eXtended finite element method implementation in COMSOL Multiphysics: solid mechanics', *Finite Elements in Analysis and Design*, vol. 202.
- Jafari, A, Vahab, M & Khalili, N 2021a, 'Fully coupled XFEM formulation for hydraulic fracturing simulation based on a generalized fluid leak-off model', *Computer Methods in Applied Mechanics and Engineering*, vol. 373.
- Jafari, A, Vahab, M, Broumand, P & Khalili, N 2021b, 'An eXtended finite element method implementation in COMSOL Multiphysics: thermo-hydro-mechanical modeling of fluid flow in discontinuous porous media', arXiv preprint arXiv:2112.11918.
- Khalili, N & Selvadurai, APS 2003, 'A fully coupled constitutive model for thermo-hydro-mechanical analysis in elastic media with double porosity', *Geophysical Research Letters*, vol. 30, no. 24.
- Khoei, AR, Moallemi, S & Haghghat, E 2012, 'Self-similar solutions for elastohydrodynamic cavity flow', *Proceedings of the Royal Society of London A, Mathematical and Physical Sciences*, vol. 400, no. 1819, pp. 289–313.
- Spence, DA & Sharp, P 1985, 'Self-similar solutions for elastohydrodynamic cavity flow', *Proceedings of the Royal Society of London A: Mathematical and Physical Sciences*, vol. 400, no. 1819, pp. 289–313.
- Terzaghi, K, Peck, RB & Mesri, G 1996, *Soil Mechanics in Engineering Practice*, John Wiley & Sons, Hoboken.
- Vahab, M, Hirmand, MR, Jafari, A & Khalili, N 2021, 'Numerical analysis of multiple hydro-fracture growth in layered media based on a non-differentiable energy minimization approach', *Engineering Fracture Mechanics*, vol. 241, p. 107361.
- Zhou, S, Rabczuk, T & Zhuang, X 2018, 'Phase field modeling of quasi-static and dynamic crack propagation: COMSOL implementation and case studies', *Advances in Engineering Software*, vol. 122, pp. 31–49.
- Zienkiewicz, OC, Chan, AHC, Pastor, M, Schrefler, BA & Shiomi, T 1999, *Computational Geomechanics*, Wiley, Chichester.